An Adaptive Meshing Approach to Capture Hydraulic Fracturing

Omidi, O. and Abedi, R.
Department of Mechanical, Aerospace & Biomedical Engineering, The University of Tennessee Space Institute, TN, USA

Enayatpour, S.
Center for Petroleum and Geosystems Engineering, The University of Texas at Austin, TX, USA

ABSTRACT: Hydraulic fracturing is widely employed to stimulate oil and gas reservoirs to increase the productivity of these naturally fissured rock domains. Different numerical techniques are available to examine how hydraulic fractures propagate. They are mainly categorized into continuum and interface-based methods. Cohesive models are among the most effective class of interfacial approaches representing crack surfaces as sharp material interfaces. In lieu of a traditional cohesive model, we have formulated and employed an interfacial damage model that incorporates the processes of nucleation, growth and coalescence on the fracture surfaces. Utilizing a dynamic adaptive meshing, we employed a Spacetime Discontinuous Galerkin (SDG) finite element method to simulate hydraulic fracture propagation. Our SDG implementation adaptively aligns the element boundaries with crack-path trajectories that are obtained as a part of the solution according to a crack growth criterion. Thus, this model does not suffer the mesh-dependent effects encountered in most other numerical fracture models. Furthermore, no discontinuous features are introduced within the elements as opposed to XFEM and generalized finite element methods. Adaptive mesh refinement in an area allows free nucleation, growth and branching of cracks oriented arbitrarily in the domain without any mesh bias whereas a coarse mesh can be used in other regions of the domain to utilize an efficient implementation. Presenting numerical examples, we performed a sensitivity analysis of some input variables such as the magnitude of *in-situ* stress components, number and orientation of induced fractures is performed to demonstrate the effectiveness of our approach in resolving hydraulic fracturing.

1 Introduction

Enhancing production from shale and other tight formations has become one of the main challenges in oil industry. Since these formations have extremely low permeability and low porosity, the technique of hydraulic fracturing is widely employed as a treatment to increase production rates. Hydraulic fracturing treatment being rapidly developed has changed the energy industry throughout the world. Understanding how fractures initiate and propagate from wellbores is necessary to efficiently perform such a costly treatment. Wellbores are commonly perforated in wells with cemented liners before hydraulic fracturing is carried out. This approach is called the plug-and-perf stimulation technique. Perforation plays the role of a fracture initially induced to control crack initiation and its propagation direction into the reservoir. Utilizing perforations as single fractures from the wellbore toward the reservoir can avoid multiple and reoriented fractures from a wellbore. A successful treatment via hydraulic fracturing to get better propagation pattern highly depends on different parameters including the length and orientation of the perforations, the magnitude of *in-situ* stress components known as stress anisotropy in the plane fracturing occurs.

There have been many attempts to numerically capture fracture propagation in tight formations during hydraulic fracturing process [1]. The cracking process in rock is distinct from cracking of other materials, such as metal and glass, in which it is not a sudden onset of new free surfaces, but continuous forming and connecting micro-cracks. Besides, hydraulic fracture propagation is governed by coupling of fluid flow and crack faces, which makes it a very complex problem. Numerical simulation is a useful tool to understand the governing mechanisms in which the energy is dissipated while the cracks are propagated in the reservoir. Several approaches mainly categorized into discrete and continuum methods are available to address the challenges in a hydraulic fracturing simulation. Since rocks are

categorized as a type of granular materials, Discrete Element Method can be possibly used for the crack propagation study [2, 3]. Although much effort has been devoted to the development of continuum-based damage model (CDM) for rock in the recent years, there are a few studies in which a CDM is employed in a hydraulic fracturing simulation [4, 5]. Developing a continuum failure model for dynamic fracture and post fracture responses of porous rocks, Shojaei *et.al.* investigated the hydraulic fracture growth in a reservoir rock [4]. They employed the model incorporating plasticity and damage mechanisms to study the effect of injected pore fluid in development of fracture surfaces in a hydraulically fractured rock.

Sharp discontinuities can be either implemented between adjacent elements [6] or within elements, as in the eXtended FEM [7, 8, 9], Generalized FEM [10, 11] or other methods with embedded strong discontinuities. The basic idea of XFEM/GFEM is to use a partition of unity to build finite element shape functions. Cohesive models are among the most effective class of discrete methods representing crack surfaces as sharp material interfaces between adjacent elements [12, 13]. The XFEM, which was proposed by Belytschko and co-workers [7, 8, 9], has been widely used for crack growth simulation. It has been used very successfully to model cracks because the finite element mesh can be created independent from the crack geometry, and in particular the domain does not have to be re-meshed as the crack propagates. In the XFEM, the fracture is propagated independently of the mesh structure by permitting it to cross the elements. However, alleviating the drawbacks associated with traditional approaches that require meshing cracked surfaces and updating the mesh for a growing crack, the XFEM has limitations in hydraulic fracturing simulations such as not capturing crack branches which is probable in a dynamics crack growth mechanism. Focusing on propagating fractures with complex geometries, like those encountered in early stages of hydraulic fracturing, Gupta and Duarte proposed a GFEM for the simulation of non-planar 3D hydraulic fractures [14]. In their proposed GFEM, the representation of fracture surfaces is independent of the volume FE mesh and consequently, complex surface features like sharp turns and kinks can be accurately represented [14].

The unconventional gas reservoirs exhibit tremendous amount of both small-scale and large-scale heterogeneity, with pre-existing natural fractures/weak planes. Recently some numerical research works have been carried out for hydraulic fracturing in these naturally fractured formations. Dahi-Taleghani and Olson used the XFEM in their two-dimensional model and addressed these issues [15]. They used critical energy release rate ratio as the criterion for interaction between the hydraulic fracture and the natural fractures [16]. Most hydraulic fracture models are based on linear elastic fracture mechanics (LEFM) while a better choice for fracture propagation is to utilize a cohesive zone model. Some applications of cohesive zone models for the analysis of hydraulic fractures include the work of Chen *et.al.* [12], Carrier and Granet [13] and Mohammadnejad and Khoei [17]. Mohammadnejad and Khoei employed the XFEM for hydraulic fracture propagation by developing a coupled numerical tool [17].

2 Spacetime Discontinuous Galerkin FEM

2.1 Spacetime discretization

Meshing, which is discretization of the domain into elements with pairwise disjoint interiors, is an important part of computational solutions in a crack propagation problem. The efficiency of the solution technique with a desirable accuracy highly depends on the number, size, polynomial order, and distribution of elements in the mesh. Herein, a spacetime discontinuous Galerkin (SDG) finite element method utilizing the simultaneous discretization of both space and time is developed to numerically simulate wave propagation into a domain as a time-dependent phenomena for mechanical stress in materials. Therefore, an efficient mesh of the spacetime domain of interest is necessary to secure a sufficiently accurate numerical solution for such a hyperbolic partial differential equations (PDEs) in space and time variables.

In this study, a specialized algorithm developed by Abedi *et.al.* to mesh directly in spacetime is used to address an efficient SDG solution [18]. Their advancing front algorithm called Tent Pitcher incrementally constructs an unstructured spacetime mesh by considering certain geometric constraints. They showed how to adapt the mesh resolution to numerical error estimates, in $2d\times$time. A significant feature of the utilized algorithm is to adaptively refine and coarsen the mesh in spacetime that improves the overall efficiency of the simulation in solving wave propagation particularly with a nonlinear physics such as fracture.

This SDG solver works with unstructured *causal* spacetime meshes as shown in Figure 1 as a simple $1d\times$time noncausal mesh. The inclined arrows indicate the characteristic directions where it is assumed the maximum wave speed is equal for the left- and right-moving waves. We impose a causality constraint on all facets in the spacetime mesh enabling a local solution scheme. The asymmetric causality dependency generates a partial element ordering by which the global solution can be computed locally, one element at a time. For example, the solution of element C depends only on the solution of earlier elements A and B because the inflow facets shown in red are shallower than the maximum wave speed. The solutions of A and B, however, do not de-
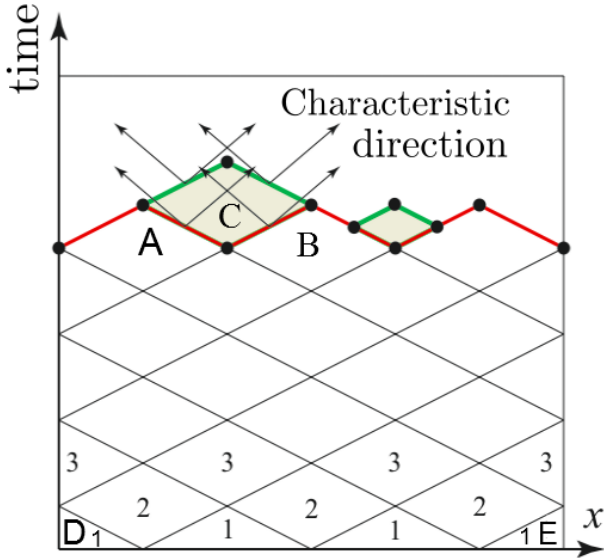
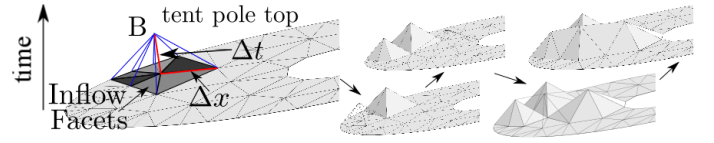Figure 1: SDG local solution scheme on a causal spacetime mesh

Figure 2: Tent pitching in spacetime

2.2 Adaptive spacetime meshing

The local spacetime structure of the SDG solver enables a powerful approach to dynamic adaptive meshing. An error indicator is computed for each new patch solution. If the error is acceptable, the patch solution is accepted and stored for use as inflow data for subsequent patches. If the error is too large, the patch is rejected and the solver passes a demand for mesh refinement to the meshing code. If the error is too small, the patch is accepted and a request for subsequent mesh coarsening is issued. Adaptive Tent Pitcher responds to refinement demands by refining the front mesh before restarting the patch-generation procedure. This generates corresponding refinement in the spacetime mesh. In $2d \times$ time, we implement common adaptive meshing operations, such as vertex-deletion, edge flips, and vertex motion, as special spacetime patches (see Figure 3). This contrasts with the instantaneous mesh modifications applied between time steps in conventional adaptive meshing algorithms that require expensive and error-prone projections of the solution from the old mesh onto the new mesh. Since the special SDG patches conform to both the old front mesh on their inflow facets and to the new front mesh on their outflow facets, no solution projection is needed, and high-order accuracy is preserved.

We can achieve strong, dynamic refinement because the adaptive meshing and the patch solutions are local operations that share the same granularity within the SDG algorithm. This contrasts with conventional adaptive methods, where remeshing is typically a global operation that is only applied after several time steps have been computed. SDG adaptive meshing closely tracks dynamic solution features, such as the trajectories of multiple wavefronts in a crack-tip wave scattering model.

The use of adaptive meshing allows free nucleation and extension of fracture interfaces. Hence, the fracture interfaces can be aligned with crack path trajectories that are located and oriented arbitrarily in the domain[6]. Furthermore, adaptive meshing also enables mesh refinement in regions with complex features such as crack nucleation, growth, and branching whereas a coarse mesh can be used in other regions of the domain to make the implementation efficient. The key feature here is the local spacetime structure of the SDG solver which makes dynamic adaptive meshing possible as a powerful technique. An error indicator is

pend on C. The level-1 elements depend only on initial conditions and boundary conditions for the elements D and E. The level-1 element solutions can be computed locally and in parallel. Thus, causal SDG meshes enable asynchronous, element-by-element solutions with linear complexity.

In practice, we replace the individual elements with small clusters of simplex elements called *patches*, where only the exterior patch facets need to be causal; see Figure 2 for clusters of tetrahedral elements in $2d \times$ time. We implement an advancing-front meshing/solution procedure. The *Tent Pitcher* algorithm [6] generates a sequence of causal spacetime patches, and we solve each one as soon as it is generated. Using an advancing-front procedure, in each step the *Tent Pitcher* algorithm advances in time a vertex in the *front mesh* to define a local front update; the causality constraint limits the maximum time increment Δt at the vertex. A small mesh of spacetime simplices covers the region between the old and new fronts to form a new patch. We solve new patches as local problems and update the current front, until the entire spacetime analysis domain is solved. This feature contrasts our SDG method with other common spacetime DG methods where elements arranged in spacetime slabs are coupled through their noncausal facets and solved simultaneously. For more details of the SDG formulation for linear elastodynamics see [18]. As mentioned before, superior performance in resolving shocks and other sharp solution features, element level balance properties, support for nonconforming meshes and arbitrary spatial polynomial order, that lead to very flexible hp-adaptive schemes, are a few of the advantages of DG methods over continuous FEMs.
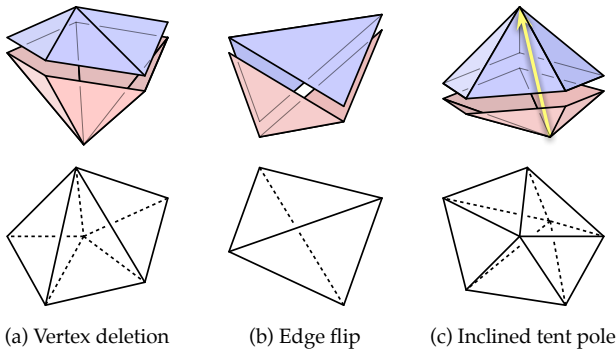
(a) Vertex deletion   (b) Edge flip   (c) Inclined tent pole

Figure 3: Adaptive meshing operations via special space-time patches (top) vs. conventional $2d$ remeshing operations (bottom)

(a) Bulk damage   (b) Fixed mesh

(c) Adaptive mesh   (d) XFEM

Figure 4: Discretization schemes for tracking cracks in the FEM

computed for each new patch solution. If the error is acceptable, the patch solution is accepted and stored for use as inflow data for subsequent patches. If the error is too large, the patch is rejected and the solver passes a demand for mesh refinement to the meshing code. If the error is too small, the patch is accepted and a request for subsequent mesh coarsening is issued. The adaptive Tent Pitcher software responds to refinement demands by refining the front mesh before restarting the patch-generation procedure. This produces corresponding refinement in the spacetime mesh.

Some distinct aspects of the SDG method are:

- Local-effect adaptivity: Rejection of elements with large error does not require reanalysis of the entire domain as needed for implicit time marching methods.

- Arbitrary order and size in time: The spatial element size adjustment in h-adaptive schemes is a major source of geometry-induced stiffness, which can drastically affect the performance of time marching schemes. To avoid temporal resolution errors dominating the overall accuracy and efficiency, the ability to achieve arbitrary and spatially variant temporal order of accuracy is highly desired in adaptive simulations.

- Spacetime adaptive operations: Transient problems often involve sharp moving fronts in spacetime. While the majority of adaptive methods are concerned with adjusting the spatial mesh at the initial time a fully efficient adaptive scheme requires simultaneous adaptive operations in spacetime.

2.3 Adaptive strategy for tracking cracks

Four commonly-employed crack tracking strategies are illustrated in Figure 4. These are based on the Finite Element Method as the widely-used numerical technique app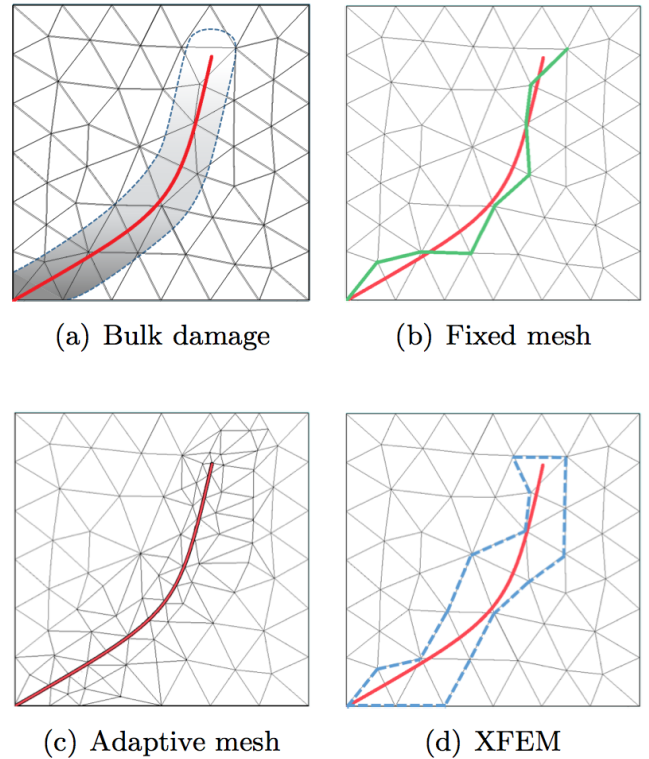lied to fracture problems. By using a continuum damage model (*i.e.* Figure 4(a)), the crack can be tracked with an appropriate mesh size in damaged regions to capture a localized path. However, it does not capture physical crack faces and can only represent a macro-cracking path along with its associated degradation caused by cracking. Therefore, this approach is not appropriate for hydraulic fracturing. The other possibility for the crack tracking is to utilize a fixed discretization (*i.e.* Figure 4(b)) while interface elements are inserted on a predefined crack path along which the crack is assumed to propagate when a load is applied. Obviously, handling of mixed mode loadings, where the crack path is not predictable, is challenging and particularly the crack path speed with a fixed mesh is not reliable. A usual alternative to the fixed mesh strategy is the use of adaptive meshing scheme as illustrated in Figure 4(c) in which the evolution of the crack path is successfully followed. Simulating crack growth using the classical FEM is quite difficult because the topology of the domain changes continuously. On the other hand, allowing to simulate arbitrary discontinuity with a fixed mesh, the XFEM method (*i.e.* Figure 4(d)) follows a crack path within the elements and in particular the domain does not have to be re-meshed as the crack propagates. Although the XFEM alleviates the problem of modeling arbitrary cracks and discontinuities of the finite element mesh, the available XFEM implementations are mostly limited to the linear elastic fracture mechanics
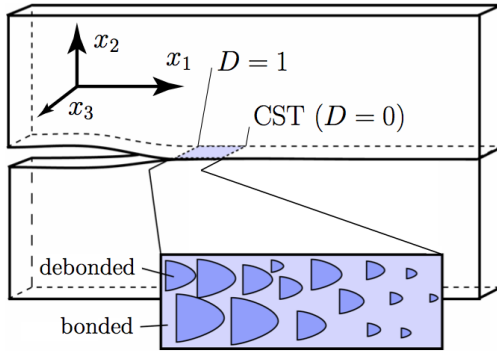
Figure 5: Cohesive process zone and the crack propagation mechanism

(LEFM) framework. Due to many technical issues, it is quite difficult to close the gap between complex LEFM and the study of cracks considering nonlinear mechanisms such as plasticity and damage.

Figure 5 illustrates an active, fully developed fracture process zone in the employed interfacial-damage cohesive model. The cohesive surface tip (CST) is the leading edge of the cohesive process zone where interfacial damage begins to accumulate from $D = 0$ until complete damage, $D = 1$, is attained at the trailing edge of the process zone.

The crack propagation criterion is tested every time a patch is pitched over an active CST vertex, such as A in Figure 6. Vertex A may be the tip of an advancing crack as illustrated in the figure or be a newly nucleated CST. In general, no two crack edges around a common vertex are permitted to have a relative angle smaller than a user-specified tolerance in the SDG implementation; otherwise, the acute angle generated may introduce errors in the discrete finite element solution. The occurrence of such instances, other than the aforementioned shielding for the crack propagation, is very infrequent and is limited to cases where one crack collides with another crack on its trailing edges or at its CST.

An active CST will be examined for propagation directions every time the vertex is advanced in time by pitching a tent. Once the propagation criterion yields a nonzero number of propagation directions, the vertex is no longer inspected for crack growth. The requested crack paths on the vertex are in turn achieved by manipulations to the space mesh as shown below. The CST flag of the vertex is inactivated after all the requested propagation paths are achieved.

Figure 6(a) illustrates a patch, where the CST vertex A is erected to A'. As demonstrated, the propagation criterion yields one extension direction after the patch is solved. Typically, the propagation angle is not aligned with any of the element boundaries. Herein, propagation direction passes through element e. We manipulate the space mesh in a way
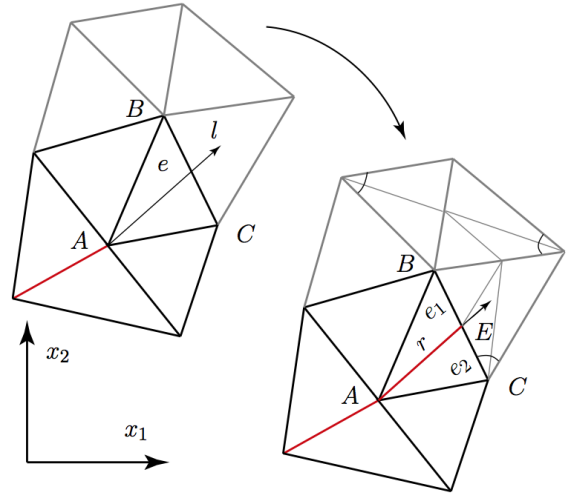
(a) CST insertion on the opposite edge of the CST by a refinement operation.
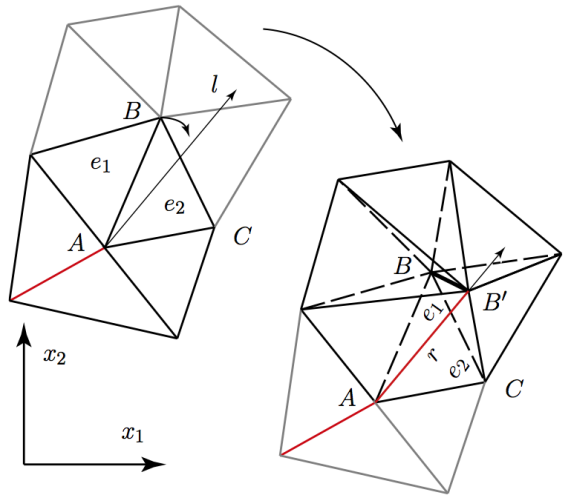
(b) The spatial transition of a vertex by a tent pitching operation.

Figure 6: Extension of a crack in the space mesh through refinement and tent pitching operations

that the edge, r, between the two triangles e_1, e_2 connected to the CST is aligned with the propagation direction. There are two approaches to introduce an element boundary along the crack direction.

In Figure 6(a), the vertex E is inserted on the edge BC such that AE is aligned with the crack direction. Subsequently, the space element e is subdivided to elements e_1 and e_2. This operation is similar to the edge bisection procedure employed to refine the element e. The refinement in element e will instigate a series of refinements according to the newest-vertex bisection algorithm on neighboring element in the space mesh to preserve the conformal structure of the space mesh. For example, the chain for refinement is propagated to three elements in the figure.

Figure 6(b) shows a situation where the direction of the element boundary AB is close to the requested crack direction, l. We align the edge AB with the crack direction by moving the vertex B to a point on line l. This can be achieved by erecting a tilted tent pole on vertex B such that the top vertex B' lies on line l. If the patch is accepted, we update the front and activate the cohesive flag of the edge AB'. As opposed to previous approach, the propagation direction is not achieved immediately and an intermediate tent pitching is involved. In fact, the move of the vertex B to line l may not be achieved in one step. In many instances the process may take several pitches on vertex B and subsequent tent pole tops; the tent pole top gets closer to the line l each time a patch is erected, until the element edge is aligned with the crack.

3 Numerical Results

In this section, two examples are presented to demonstrate the performance of our SDG approach for 2D simulations of hydraulic fracturing. The focus of the applications discussed herein is on the shale gas reservoirs in which fracturing occurs in depths with low permeability. However for such a very tight formation, the leak-off of fluid across crack faces can be neglected. Besides, low viscosity fracturing fluids such as treated water is common nowadays in the hydraulic fracturing. In these conditions, the fluid pressure along fracture faces, specifically near the wellbore can be treated as a nearly constant due to the high *in-situ* stresses acting as effective confining pressures in the deep reservoirs and the low fluid viscosity. Utilizing analytical solutions for this problem, references [19, 20] showed that considering this behavior is reasonable. Allowing that, it is also practical to deduce that the fluid and fracture fronts occur simultaneously and are coincident, which means the fluid lag is negligible. It should be noted that the size of the fluid lag is inversely proportional to σ_0^3, in which σ_0 is the far field confining stress [21].

As the first problem, we simulate a single fracture whose faces are subjected to an internal pressure. This kind of simulation has been widely covered by many researchers in the literature. By the way, in order to isolate the well from undesirable regions and to consider some operational considerations in the field along with stability concerns, wellbores usually are cased and then perforated in the reservoir with cemented liners where the plug-and-perf stimulation technique is commonly employed. Accordingly it is more practical to perform the hydraulic fracture operation through perforations. Therefore, the next problem followed in this paper is devoted to the hydraulic fracturing from the oriented perforations. In the following, the maximum and minimum compressive stresses are denoted as σ_H and σ_h, respectively.

3.1 Single pressurized fracture

A pressurized crack with vertical orientation in a domain, which is subjected to far field confining stresses as bi-axial tractions, is considered in the following examination. As mentioned above, a constant pressure is applied to the crack faces while fractures propagate. The initial crack has a half length of 0.02 m and is subjected to confining *in-situ* stresses: $\sigma_h = 2.425$ MPa and $\sigma_H = 4.85$ MPa. The initial fracture is oriented 90° with respect to the horizontal plane which is parallel to the direction of σ_H. The material properties are: Young's modulus $E = 20$ GPa and Poisson's ratio $v = 0.2$. The fluid pressure is assumed to increase in time as a dynamic loading from a stabilizing constant pressure being applied as a static load. The crack patterns obtained for two different time steps are illustrated in Figure 7. The crack propagates rather in a straight line before it branches ahead of the initial crack tip.

3.2 Hydraulic fracturing from oriented perforations

Perforations in a hydraulic fracturing treatment play the role of a transmission channel between the wellbore and the reservoir. In fact, a perforation may serve as an initial fracture to help with crack nucleation and slightly force propagation direction to perform an efficient treatment. Therefore, perforations are important in the complex fracture geometries around wellbore. Having a single fracture initiated from a wellbore is one of the main objectives of creating the perforations as a technique to avoid multiple T-shaped and reoriented fractures. However, the success of stimulation treatment through perforations depends on several parameters including its length, diameter along with permeability of the rock around the perforation. The enhanced permeability of the rock around the wellbore controls recovery flow through a perforation. By shortly reviewing effective
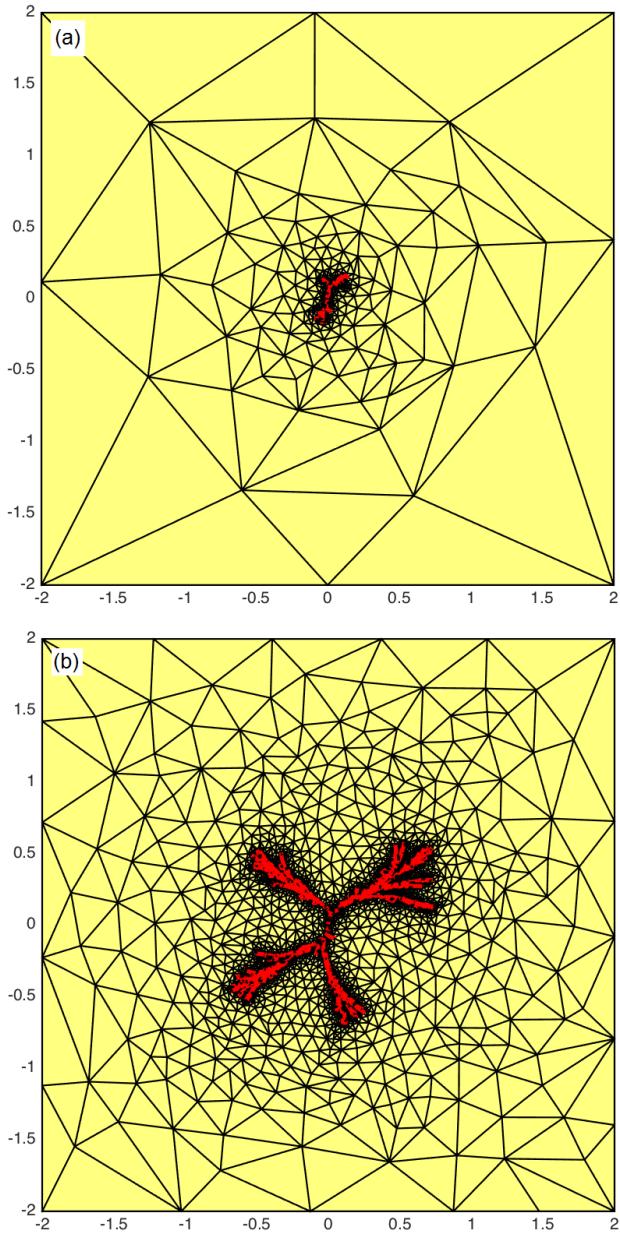
Figure 7: Crack propagation on the space mesh in single pressurized fracture
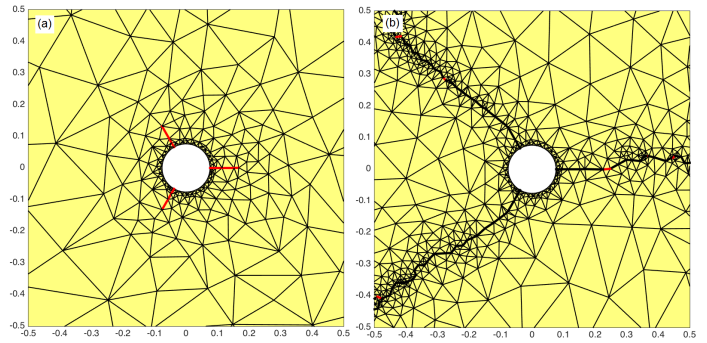

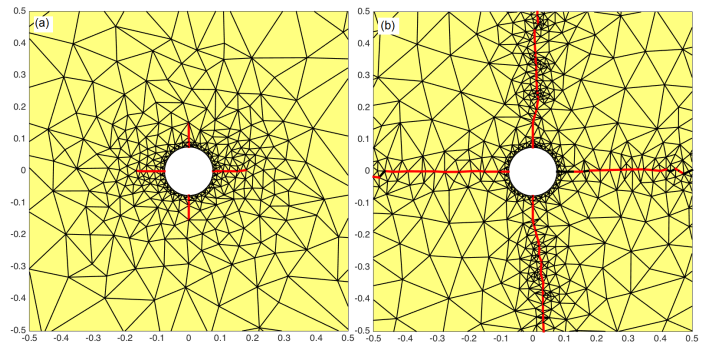Figure 8: Crack propagation on the space mesh in the three-perforation case

Figure 9: Crack propagation on the space mesh in the four-perforation case

parameters, which are important for a perforation design, the function of perforation in hydraulic fracturing is discussed in the following. Perforation phasing, which is the angle between the two successive perforations, is another important parameter affecting production rate and needs to be carefully assessed at its design stage. Among many possible angles, common perforation phasing angles are 60°, 90°, 120° and 180°. Herein, one application with three different phasing angles of 60°, 90°, 120° are considered.

To study the efficacy of perforation patterns, we are looking into three scenarios. Figure 8 shows three perforation points at 0, 120, and 240 degrees around the wellbore. As expected, the first fracture starts to emanate from the perforation placed at 0 degrees because the minimum horizontal stress is perpendicular to this fracture. The continuation of fracturing orders in Figure 8 does not show any preference in terms of starting from which perforation, therefore, they continue to grow almost simultaneously. Since all the three fractures, eventually grow and exhibit the most ramified pattern, we conclude that this pattern of three perforations is an efficient pattern to start hydraulic fracturing.

Figure 9 shows the case of four perforations equally phased around the casing. Similar to previous case, fracture creation starts at the perforations placed at 0 and 180 de-
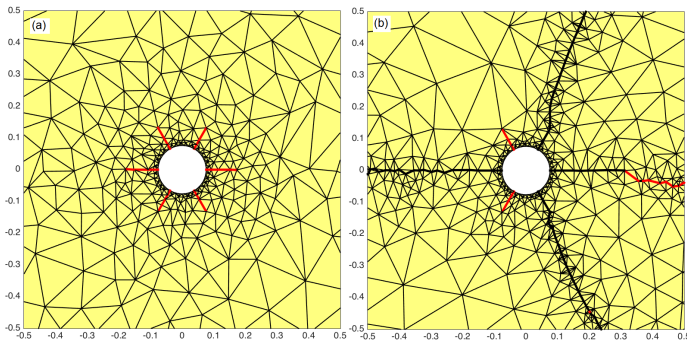
Figure 10: Crack propagation on the space mesh in the six-perforation case

grees due to the direction of the minimum *in-situ* stress being normal to these two fractures. After they open and grow longer, the other two fractures at 90 and 270 degrees obtain the potential to grow simultaneously. Figure 10 shows an interesting result that confirms the two previous patterns and justifies the use of a maximum number of four perforations for hydraulic fracture creation. The fracture stage in Figure 10(b), shows that the first two fractures that start to grow are the ones at 0 and 180 degrees, after that, since there is no preference of growth (except for the material strength which due to random distribution of properties, in this case seems to be lower on the right half) between the set of two perforations on the right and two perforations on the left quadrants, the ones on the right start to grow first. This result indicates that in this case of six perforations, two perforations remain unused and we recommend a maximum of four perforations in cross section of casing to obtain the best fracture creation results.

4 Conclusions

One of the most important applications of hydraulic fracturing nowadays is to improve the recovery of unconventional hydrocarbon reservoirs. Having an appropriate fracture propagation model in rocks is a crucial issue for a hydraulic fracture design. Many approaches have been developed to efficiently perform crack growth simulations, which are mostly based on either efficient remeshing techniques or the XFEM/GFEM employing fixed meshes, but these are mainly limited to the linear elastic fracture mechanics (LEFM) framework. In this paper, an interfacial damage model implemented in a Spacetime Discontinuous Galerkin (SDG) framework is utilized to simulate nucleation and then propagation of hydraulically induced fractures in an oil reservoir. The SDG method offers many advantages over conventional and extended/generalized finite element methods including dynamic adaptive meshing, interface tracking, and element-wise conservation. To facilitate crack propagation in any arbitrary direction we use the SDG's powerful adaptive meshing capabilities to align cracks with inter-element boundaries; Unlike X-FEM methods no special discontinuity functions are required.

Although hydraulic fracturing has been employed for several decades in oil industry, a thorough understanding of the interaction between induced hydraulic fractures and pre-existing natural fractures is still challenging. Our approach is applicable to hydraulic fracturing where an induced major crack propagates and intersects natural fractures which in turn are hydraulically loaded and extended to intersect other fissures resulting in a complicated fracture network. Furthermore, incorporation of macro-micro crack interactions can explain discrepancies for tracking efficiency between real productivity and computational estimations. The future work focuses on utilizing the developed interfacial damage model in capturing the interactions between hydraulically induced fractures and natural fractures.

Besides, stochastic distribution of material defects plays a critical role in fracture processes, particularly in brittle materials such as rocks. The failure initiated at these weaker sites is often accelerated through increasing stress concentrations induced by initial fracture growth and local inhomogeneity. The energy absorption and stress release through these local features shields surrounding regions and results in a very non-uniform failure pattern at mesoscale. Deterministic continuum models treating the material as perfectly homogeneous predict simultaneous failures at regions of high stress, which is not physical. Unfortunately, these problems are somehow shadowed in discrete setting due to slight inhomogeneities implied by numerical errors and often finite loci where cracks can propagate. To address this issue at the continuum level, a probabilistic nucleation model can be devised where cracks nucleate from defects that are randomly distributed in the bulk. This topic can also be the future continuation of this stream of research.

References

[1] Adachi, J.I., E. Siebrits, A. Peirce, and J. Desroches (2007) Computer simulation of hydraulic fractures. *International Journal of Rock Mechanics and Mining Sciences*, **44**, 739–757.

[2] Galindo Torres, S.A. and J.D. Muñoz Castaño (2007) Simulation of the hydraulic fracture process in two dimensions using a discrete element method. *Phys. Rev. E*, **75**, 066109.

[3] Zhao, Q., A. Lisjak, O. Mahabadi, Q. Liu, and G. Grasselli (2014) Numerical simulation of hydraulic fracturing and associated microseismicity using finite-

discrete element method. *Journal of Rock Mechanics and Geotechnical Engineering*, **6**, 574–581.

[4] Shojaei, A., A. Dahi-Taleghani, and G. Li (2014) A continuum damage failure model for hydraulic fracturing of porous rocks. *International Journal of Plasticity*, **59**, 199–212.

[5] Busetti, S., K. Mish, P. Hennings, and Z. Reches (2012) Damage and plastic deformation of reservoir rocks: Part 2. propagation of a hydraulic fracture. *AAPG Bulletin*, **96**, 1711–1732.

[6] Abedi, R. (2010) Spacetime damage-based cohesive model for elastodynamic fracture with dynamic contact. Ph.D. dissertation, Department of Theoretical and Applied Mechanics, University of Illinois at Urbana–Champaign.

[7] Belytschko, T. and T. Black (1999) Elastic crack growth in finite elements with minimal remeshing. *International Journal for Numerical Methods in Engineering*, **45**, 601–620.

[8] Moes, N., J. Dolbow, and T. Belytschko (1999) A finite element method for crack growth without remeshing. *International Journal for Numerical Methods in Engineering*, **46**, 131–150.

[9] Dolbow, J., N. Moes, and T. Belytschko (2000) Discontinuous enrichment in finite elements with a partition of unity method. *Finite Elements in Analysis and Design*, **36**, 235–260.

[10] Strouboulis, T., I. Babuška, and K. Copps (2000) The design and analysis of the generalized finite element method. *Computer Methods in Applied Mechanics and Engineering*, **181**, 43–69.

[11] Strouboulis, T., K. Copps, and I. Babuška (2001) The generalized finite element method. *Computer Methods in Applied Mechanics and Engineering*, **190**, 4081–4193.

[12] Chen, Z., A.P. Bunger, X. Zhang, and R.G. Jeffrey (2009) Cohesive zone finite element-based modeling of hydraulic fractures. *Acta Mechanica Solida Sinica*, **22**, 443–452.

[13] Carrier, B. and S. Granet (2012) Numerical modeling of hydraulic fracture problem in permeable medium using cohesive zone model. *Engineering Fracture Mechanics*, **79**, 312–328.

[14] Gupta, P. and C.A. Duarte (2014) Simulation of nonplanar three-dimensional hydraulic fracture propagation. *International Journal for Numerical and Analytical Methods in Geomechanics*, **38**, 1397–1430.

[15] Dahi-Taleghani, A. and J.E. Olson (2011) Numerical modeling of multistranded-hydraulic-fracture propagation: Accounting for the interaction between induced and natural fractures. *SPE Journal*, **16**, 575–581.

[16] Dahi-Taleghani, A. and J.E. Olson (2014) How natural fractures could affect hydraulic-fracture geometry. *SPE Journal*, **19**, 161–171.

[17] Mohammadnejad, T. and A.R. Khoei (2013) An extended finite element method for hydraulic fracture propagation in deformable porous media with the cohesive crack model. *Finite Elements in Analysis and Design*, **73**, 77–95.

[18] Abedi, R., R.B. Haber, and B. Petracovici (2006) A spacetime discontinuous Galerkin method for elastodynamics with element-level balance of linear momentum. *Computer Methods in Applied Mechanics and Engineering*, **195**, 3247–3273.

[19] Gordeliy, E. and A. Peirce (2013) Implicit level set schemes for modeling hydraulic fractures using the XFEM. *Computer Methods in Applied Mechanics and Engineering*, **266**, 125–143.

[20] Detournay, E. (2004) Propagation regimes of fluid-driven fractures in impermeable rocks. *International Journal of Geomechanics*, **4**, 35–45.

[21] Lecampion, B. and E. Detournay (2007) An implicit algorithm for the propagation of a hydraulic fracture with a fluid lag. *Computer Methods in Applied Mechanics and Engineering*, **196**, 4863–4880.